

# Evaluation of first-principles techniques for obtaining materials parameters of $\alpha$ -uranium and the (001) $\alpha$ -uranium surface

Christopher D. Taylor

*Los Alamos National Laboratory, Los Alamos, New Mexico 87545, USA*

(Received 2 November 2007; revised manuscript received 14 January 2008; published 17 March 2008)

First-principles calculations based on the projector augmented-wave (PAW) technique have been applied to the prediction of materials properties of  $\alpha$ -uranium and its (001) surface. The results of the PAW calculations are shown to be comparable in accuracy to the full-potential calculations reported elsewhere. In addition to calculating lattice constants and elastic moduli, the vacancy formation energy (1.95 eV), (001) surface relaxation ( $-3.5\%$  for  $\delta_{12}$  and  $+1.2\%$  for  $\delta_{23}$ ), (001) surface energy ( $1.4 \text{ J/m}^2$ ), and (001) work function (3.6 eV) were also obtained. The overall agreement with experiment is satisfactory. Using an elastic model for brittle-crack failure, a yield stress of 430 MPa was estimated. Further exploration of materials failure modes (such as plastic deformation) awaits a larger-scale atomistic treatment. Full spin-orbit and scalar relativistic calculations were shown to give results with similar levels of accuracy compared to experiment.

DOI: [10.1103/PhysRevB.77.094119](https://doi.org/10.1103/PhysRevB.77.094119)

PACS number(s): 61.66.Bi, 71.15.Mb, 68.35.Md, 68.35.B-

## INTRODUCTION

The first-principles modeling of materials promises to revolutionize the way materials are designed, used, and maintained.<sup>1</sup> In order for this ideal to be realized, simulation techniques must be fast, accurate, and well tested. Since phenomena in materials typically occur at multiple time and length scales, the current philosophy is to develop simulation techniques that couple together physics on multiple levels. Hence, the term “multiscale modeling” is often used. This may mean, for example, that results from simulations obtained at an electronic-atomic scale level are then “fed into” simulations operating at an atom-atom pair-potential level, and from thence into continuum models.<sup>2</sup>

Clearly, when the physics of the material at the atomistic level becomes more challenging, it is more difficult to create such a comprehensive multiscale model. The actinide elements, for example, are among the most challenging atomic systems known due to the requirement for considering the effects of strong correlation in the electronic structure. Recently, electronic structure calculations have appeared for these elements with varying degrees of success in capturing the structural and mechanical properties of these materials. Using the full-potential linear muffin tin orbital technique, for example, Söderlind calculated the structural and elastic properties of orthorhombic  $\alpha$ -uranium.<sup>3</sup> The calculated lattice constants had an accuracy of approximately 1% compared to the experimental values (determined at 40 K).<sup>4</sup> The elastic constants were much harder to model and compare with experiment, partially because unrelaxed calculations were used during the finite distortion technique and also because uranium undergoes phonon softening as a function of temperature.<sup>5</sup> The qualitative trends between the elastic constants were, however, in good agreement with the experimental values. The root-mean-square deviation of the elastic moduli,  $c_{11}$  through  $c_{66}$ , was 118 GPa. An earlier study by Crocombette *et al.*, however, using a pseudopotential technique, in which the core electrons are replaced by an effective electron-electron interaction potential, was not so accurate.<sup>6</sup> The lattice constant for the  $b$  vector of the ortho-

rhombic crystal was significantly shorter by 7% and the bulk modulus was overestimated by 58%. Calculations on the atomic electronic structure (i.e., isolated atoms and molecules, not a solid) have also been performed and the results were very sensitive to the level of correlation included in the calculation.<sup>7</sup> As larger systems were studied, however, the results were shown to be less sensitive and density functional calculations to be of comparable accuracy to the high level techniques. Uranium lies below the plutonium threshold for  $f$ -electron localization, and thus, many of the strong correlation effects are only observed at low temperature, such as the charge-density wave transitions and phonon softening.<sup>5,8</sup>

Although the full-potential calculations are able to capture the physics of the atomic and electronic interactions that dictate many of the properties of the orthorhombic uranium crystal, they are not yet of sufficient computational efficiency to allow the simulation of more complex systems (i.e., larger supercells containing crystal defects, such as vacancies, and/or impurity atoms). In order to address these properties of the material away from the perfect crystal behavior, which are ultimately useful for informing an atomistic pair-potential scheme, a method involving soft pseudopotentials would be of use. The pseudopotentials used by Crocombette *et al.*<sup>6</sup> were not soft in that high cutoff energies, greater than 2000 eV, were required for the plane-wave expansion. Furthermore, it would be advantageous to use a potential that gave better agreement with the experimental lattice constants and bulk modulus. Recently, a projector-augmented wave (PAW) method has been developed<sup>9</sup> that follows a similar derivation of Vanderbilt<sup>10</sup> Kresse and Joubert<sup>11</sup> ultrasoft pseudopotentials. A PAW for uranium has been developed by Kresse and Furthmüller<sup>12</sup> and is supplied with the VASP code. The PAWs are fitted to the full-potential electronic structure of the uranium atom; hence, it is important to test the PAW with respect to the structural and elastic properties of the uranium metal. The PAW for uranium possesses a significantly lower plane-wave energy cutoff (253 eV) than the hard pseudopotential adopted by Crocombette *et al.* (2448 eV), thus making it feasible to perform large supercell calculations designed to study materials defects, surfaces, and impurity interactions.

In this work, I evaluate the projector-augmented wave potential developed by Kresse for the orthorhombic lattice structure of  $\alpha$ -uranium, and calculate additional properties from the density functional formalism, such as the energy differences between various crystalline phases, the surface energy, vacancy formation energy, and approximations to the phonon spectrum. In order to demonstrate current capabilities for extrapolating from first-principles calculations to materials design, I have also calculated the Debye and Einstein approximations for the specific heat using the first-principles data and compare these data points with experimental values in the literature.<sup>13</sup> Furthermore, a formula derived by Hayes *et al.*<sup>14</sup> is applied to consider the elastic crack resistance of the uranium metal, which value may be compared to the ultimate strength behavior. The influence on choosing between the faster scalar-relativistic calculations (in which the relativistic effect is restricted to the core electrons) and the more time-consuming full spin-orbit calculations (in which the wave function is represented as a spinor rather than a scalar function) is also examined, and the impact on accuracy is reported.

The work presented provides a basis for future investigations using the PAW method to probe the effect of impurities on the properties of metallic uranium, the impact of lattice defects on materials properties, surface modification due to the environment and subsequent impact on materials performance, and the refinement of theoretical techniques for predicting the complex magnetic and vibrational properties of uranium and uranium compounds. Furthermore, these results will be used to develop and verify an atomistic pair potential to simulate larger-scale structural and transformational behaviors of uranium.

### COMPUTATIONAL DETAILS

The electronic structure problems related to the first-principles computation of the mechanical, structural, and materials properties described herein were solved using the efficient, parallelized electronic structure code Vienna *ab initio* simulation package (VASP).<sup>12</sup> The PAW functions for uranium supplied with VASP Version 4.6 were used without modification. The PW91 exchange-correlation functional was also adopted.<sup>15</sup> Tests of the energy convergence with respect to the  $k$ -point mesh size and energy cutoff lead to the choice of an energy cutoff of 500 eV and a gamma-centered Monkhorst–Pack  $k$ -point mesh generated using a generating length of 40 Å.<sup>16</sup> This choice of  $k$ -point mesh corresponds to a  $14 \times 7 \times 8$  mesh for the conventional four-atom orthorhombic unit cell of  $\alpha$ -uranium (Fig. 1). The resulting energies were converged with respect to energy cutoff and  $k$ -point mesh to within 2 meV (0.15 mRy). To perform relaxations, the Methfessel–Paxton smearing method was used to provide more accurate forces (width of 0.2 eV), whereas for single-point calculations, the Bloechl tetrahedron method was adopted.<sup>9,17</sup> Self-consistent electronic structure calculations were iterated to within 0.1 meV, and for geometric relaxations, iterations over the lattice positions were performed until forces were less than 0.05 eV/Å. The relaxations were performed using the conjugate gradient method.

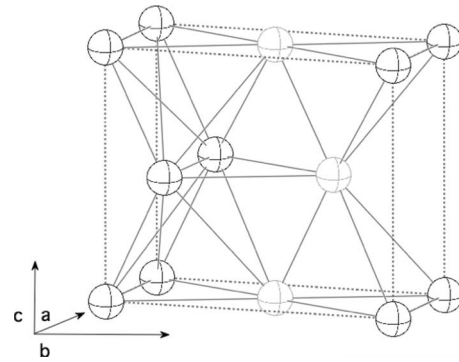


FIG. 1.  $\alpha$ -uranium four-atom conventional unit cell.

Elastic constants were calculated according to the method used by Söderlind,<sup>3</sup> with the modifications of the use of 2% distortions to eliminate “noise” due to the convergence limits used and a three-point method for evaluating the second derivatives corresponding to the lattice constants. In this method, finite distortions of various symmetries are applied to the crystal structure of  $\alpha$ -uranium and the accompanying shifts in the calculated energy. All atom positions were allowed to relax under the distortions. Using the relationship between the energy of the distortion and the distortion magnitude (0.02), it is possible to determine the elastic moduli  $c_{ij}$ . The elastic constants were then used to calculate the Debye temperature according to the application of Houston’s method derived for orthorhombic crystals.<sup>18</sup> This method can be used to determine the Debye temperature from the speed of sound in the lattice, which is determined by averaging the anisotropic speed of sound over various crystallographic directions which can be determined from a knowledge of the anisotropic elastic constants. To calculate the Einstein temperature, the vibrational modes of  $\alpha$ -uranium were estimated by performing finite-displacement calculations on a single uranium atom in a 96-atom supercell. A finite displacement of 0.01 Å and the gamma point only method were used.<sup>19</sup> The same supercell was used to calculate the vacancy formation energy. The specific heat of  $\alpha$ -uranium was calculated by combining the complementary Debye and Einstein models using the tabulated Debye function.<sup>20</sup>

Surfaces were created using the optimized lattice parameters, with full relaxation of the internal parameters and the interlayer spacings normal to the surface. The periodic slab model was used to treat the uranium surfaces. In this model, a finite number of layers of metal atoms is used to represent the semi-infinite metal, and these “slabs” are then separated by a region of vacuum thick enough to minimize the inter-slab interactions. Because only a finite number of layers is used and because this number must typically be small for the simulation to be computationally efficient, it is important to vary the number of layers required to obtain converged surface properties. Herein, I consider the variation of  $\alpha$ -uranium surface properties in the (001) direction for models consisting of between three and seven atomic layers. A  $16 \times 16 \times 1$   $k$ -point mesh was used for the primitive  $1 \times 1$  surface periodic unit cell [Fig. 2(a)]. In Fig. 2(b), I have provided a schematic of the slabmodel utilized in these calculations for a five layer slab of (001) oriented  $\alpha$ -uranium planes sepa-

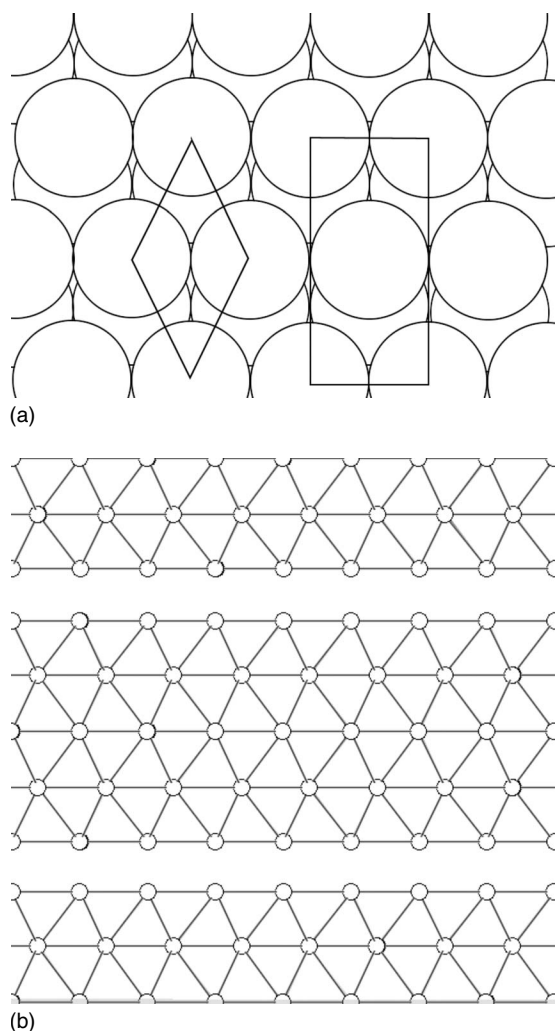


FIG. 2. (a)  $\alpha$ -Uranium  $1 \times 1$  surface periodic unit cell (left) and conventional periodic unit (right) cell in the (001) orientation. (b) Slab model used to model (001)  $\alpha$ -uranium surface with five (001) planes representing the uranium metal and vacuum separating the periodic images.

rated by a vacuum region. For calculations with the number of atomic layers  $N=3-5$ , only the outermost layer (corresponding to the distance  $d_{12}$  between the first and second atomic layers) was relaxed, whereas for  $N=6, 7$ , the two outermost layers were allowed to relax ( $d_{12}$  and  $d_{23}$ ). The inter-slab spacing was typically of the order of three to five equivalent atomic layers. The surface energy  $\gamma$  is calculated by subtracting the energy of an equivalent number of atoms in the orthorhombic structure  $NE_{bulk}$  from the energy of the surface representation  $E_{slab}$  and dividing this number by twice the surface area  $2A$  to account for the slab representation of the surface,

$$\gamma = (E_{slab} - NE_{bulk})/2A.$$

The work function  $\phi$  is obtained by subtracting the (arbitrarily referenced) Fermi level from the VASP calculation  $V_{Fermi}$  from the potential energy of the electron in the vacuum region  $V_{vac}$  obtained by a plot of the electrostatic

potential projected in the slab normal direction,

$$\phi = V_{Fermi} - V_{vac}.$$

Scalar-relativistic calculations were performed for all systems, in which case the PAW-core contribution is considered to supply the leading relativistic correction to the electronic structure. Additionally, in a number of cases, the complete spin-orbit coupling treatment was also applied, and this is stated explicitly in the tabulated data. The results are given in the following discussion (spin orbit vs scalar relativistic).

## RESULTS AND DISCUSSION

In the following sections, I present and discuss the PAW calculated lattice parameters, elastic moduli, atomic vibrational modes, Debye and Einstein temperatures, and the specific heat for the orthorhombic  $\alpha$ -uranium single crystal, making comparisons to the available experimental and theoretical data in the literature, as well as PAW calculations for other crystalline phases of uranium (fcc and bcc). The PAW calculations are shown to have comparable accuracy with the full-potential results obtained by Söderlind and to be a significant improvement upon the results obtained by Crocombe *et al.* using the hard pseudopotential. I have also calculated selected properties of the (001)-oriented single-crystal  $\alpha$ -uranium surface, and these computed properties are also compared to the best available literature data. Finally, I investigate the crack resistance of the (001) plane of the orthorhombic  $\alpha$ -uranium crystal based on the relations between the elastic modulus and the (001) surface energy.

### Lattice parameters for the crystal structures of orthorhombic $\alpha$ , face-centered cubic, and body-centered cubic uranium

The optimized lattice constants and internal parameters are presented in Table I. By inspecting the data in this table, it can be seen that the PAW calculations in both the scalar-relativistic and full spin-orbit models determine a unit cell which is somewhat smaller than that yielded by the full-potential calculations of Söderlind (Söderlind's values are  $a=2.845 \text{ \AA}$ ,  $b=5.818 \text{ \AA}$ ,  $c=4.996 \text{ \AA}$ , and  $y=0.103$ ).<sup>3</sup> The spin-orbit coupling calculations yield lattice parameters of  $a=2.797 \text{ \AA}$ ,  $b=5.867 \text{ \AA}$ ,  $c=4.893 \text{ \AA}$ , and  $y=0.098$ , which do not significantly differ from the lattice parameters determined by the scalar-relativistic method of  $a=2.800 \text{ \AA}$ ,  $b=5.896 \text{ \AA}$ ,  $c=4.893 \text{ \AA}$ , and  $y=0.097$ . These values are within 1% of the experimental values obtained at 40 K by Barrett *et al.* ( $a=2.836$ ,  $b=5.867$ ,  $c=4.936$ , and  $y=0.102$ ).<sup>4</sup> Experimental studies performed on thorium<sup>21</sup> and rare-earth metals<sup>22</sup> both indicate that variations in impurity content (typically  $\sim 50$  ppm for high purity uranium samples)<sup>23</sup> can cause variations in the measured lattice parameters of  $\sim 0.005 \text{ \AA}$ . Using this value as a guide to the accuracy of experiments for determining the lattice parameters of pure uranium, we see that none of the theoretical methods produce values that reproduce the experimental result. The PAW values underestimate the internal parameter  $y$  by about 4%. Finally, the PAW calculations significantly improve the esti-

TABLE I. Lattice constants (in Å) and internal parameters for crystalline phases of uranium calculated in both the spin-orbit formalism and scalar-relativistic treatment in the PAW approximation, compared to the results of the full-potential (FP) (Ref. 3) calculations by Söderlind, the pseudopotential calculations of Crocombette *et al.* (PP) (Ref. 6), and experiment (50 K) (Ref. 4). The volume per atom is given in Å<sup>3</sup>.

	Spin orbit	Scalar relativistic	FP	PP	Expt.
$\alpha$ -uranium					
$a$	2.797	2.800	2.845	2.809	2.836
$b$	5.867	5.896	5.818	5.447	5.867
$c$	4.893	4.893	4.996	4.964	4.936
$y$	0.098	0.097	0.103		0.102
<i>Volume/atom</i>	20.074	20.194	20.674	19.026	20.535
fcc uranium					
$a$	4.43	4.48		4.30	
<i>Volume/atom</i>	21.73	22.48		19.88	
bcc $\gamma$ -uranium					
$a$	3.43	3.43	3.46	3.37	3.47
<i>Volume/atom</i>	20.18	20.18	20.71	19.14	20.89

mate for the  $b$  parameter obtained using the pseudopotential method of Crocombette *et al.* ( $b=5.447$  Å).

The lattice constant for the fcc phase (which does not exist on the uranium phase diagram) predicted by the first-principles calculations is larger than that predicted by the pseudopotential calculations of Crocombette *et al.* The lattice constant for the high temperature bcc phase of 3.43 Å obtained by both methods for including relativistic effects (scalar-relativistic and spin-orbit couplings) is slightly lower than that obtained by experiment<sup>24</sup> (by  $\sim 1\%$ ) and yet not as low as that obtained by Crocombette *et al.* ( $\sim 3\%$  deviation from experiment).

#### Elastic moduli for $\alpha$ , face-centered cubic, and body-centered cubic uranium

After optimizing the lattice constants and internal parameters via the conjugate gradient method, the elastic moduli were calculated using the method of finite distortions, as outlined in the computational details. The resulting elastic moduli are presented in Table II. The bulk modulus, as determined from the elastic constants, is also presented in this table, as well as the root-mean-square deviation of the elastic moduli when compared with the room-temperature experimental values.<sup>25</sup> The root-mean-square deviation is provided as a means of evaluating the various techniques with respect to the full-potential model given by Söderlind.

The PAW calculations of the elastic constants are generally in good agreement with those obtained from the full-potential calculations performed by Söderlind. The spin-orbit calculations yield a closer agreement with the experimental numbers than the scalar-relativistic results, although overall the full-potential calculations by Söderlind provide the best agreement with experiment. The bulk modulus is overestimated by all the density functional methods (including this work, Söderlind's full-potential calculations and the results

of Crocombette *et al.*), with the PAW method providing a bulk modulus that falls in between the full-potential estimate and that obtained by the hard-pseudopotential calculations made by Crocombette *et al.* All theoretical methods give higher elastic moduli than the experimental evaluations made at 298 K,<sup>25</sup> an effect which can be rationalized by the temperature dependence of the atomic force constants in  $\alpha$ -uranium and actinide metals in general.<sup>5</sup> Impurity effects on the elastic constants are unknown and may possibly play a part in this variance also. This observation also concurs with the deviation in Debye temperatures between the theoretical estimates and experiment (Table III and later in the following section). From an analysis of melting temperatures, the authors of Ref. 5 determine a Debye–Waller factor for uranium of  $\theta_D=306-0.158T$ . Thus, at 0 K,  $\theta_D$  should be approximately 300 K, which is somewhat higher than the predictions made from density functional theory of 280–290 K given in Table III. For completeness, I have also provided values for the elastic moduli of the bcc and fcc phases obtained using the scalar-relativistic approximation. In agreement with the study of Söderlind, the elastic constant represented by  $C' = C_{11} - C_{12}$  is negative, indicating that these phases are mechanically unstable, with regards to the tetragonally distorted bct structure, which is not discussed herein.<sup>26</sup>

#### Debye, Einstein temperatures, and the specific heat

The set of nine elastic moduli was then applied to predict the Debye temperature for  $\alpha$ -uranium. For completeness, the Debye temperature was calculated using the values calculated from the moduli calculated in this work (PAW with spin-orbit and scalar-relativistic corrections), as well as the moduli determined from the full-potential calculations and also the experimental values.<sup>3,25</sup> To assess not only the low temperature continuum contributions to the specific heat but

TABLE II. Elastic constants,  $c_{11}-c_{66}$ , and the bulk modulus  $B$  given in gigapascals for crystalline phases of uranium calculated using the PAW method with both spin-orbit and scalar-relativistic approaches, listed with the results of the full-potential (FP) calculations given by Söderlind (Ref. 3), the pseudopotential approach of Crocombette *et al.* (PP) (Ref. 6), and experiment (298 K) (Ref. 26). The root-mean-square deviation summed over the elastic constants, relative to the experimental values (rmsd) is also given.

	Spin orbit	Scalar relativistic	FP	PP	Expt.
$\alpha$ -uranium					
$c_{11}$	293	296	300		215
$c_{22}$	227	216	220		199
$c_{33}$	331	367	320		267
$c_{12}$	60	60	50		46
$c_{13}$	30	29	5		22
$c_{23}$	147	141	110		108
$c_{44}$	149	153	150		124
$c_{55}$	117	129	93		73
$c_{66}$	95	99	120		74
$B$	147	149	130	182	115
rmsd	125	151	118		
bcc $\gamma$ -uranium					
$c_{11}$		161			
$c_{12}$		184			
$c_{44}$		56			
$B$		176		170	
fcc uranium					
$c_{11}$		184			
$c_{12}$		267			
$c_{44}$		28			
$B$		239		154	

also the higher temperature atomic vibrational contributions, the Einstein temperature was also calculated. Vibrational frequencies were calculated for a single uranium atom in a 96-atom supercell using a three-point finite difference method, and the frequencies were averaged to calculate the Einstein temperature. Together, these values are useful for the estimation of the thermodynamic properties of the material, particularly the specific heat and vibrational entropy of a solid. Table III contains both the Debye and Einstein temperatures calculated according to these methods, and in Fig. 3, the theoretical specific heat derived as a sum of Einstein and Debye contributions is plotted and compared to the data given in Ref. 13.

All three of the electronic structure methods (PAW with scalar-relativistic correction, PAW with spin-orbit calculation, and the full-potential calculations of Söderlind) overestimate the Debye temperature relative to that calculated from the experimental, room-temperature elastic constants. Clearly, the prediction of higher elastic constants from the density functional theory based methods reduces the effective Debye temperature of the simulated crystal. The Debye temperature is in fact a function of the temperature of the material, as the phonon spectrum also changes with temperature. This phenomena is called phonon softening and is believed to relate to the interaction between electrons and phonons in the solid material.<sup>5</sup> Modeling this behavior is

TABLE III. Einstein temperatures  $\theta_E$  and Debye temperatures  $\theta_D$  calculated using Houston's methods (Ref. 18). The frequencies of vibrational modes for U atoms in the lattice calculated from the electronic structure and PAW theory are also provided,  $\nu$ .

	$\theta_D$				$\theta_E$
	Spin orbit	Scalar relativistic	FP <sup>a</sup>	Expt. <sup>b</sup>	Scalar relativistic
$\alpha$ -U	281 K	287 K	288 K	251 K	138 K $\nu=79, 104, 106 \text{ cm}^{-1}$

<sup>a</sup>Reference 3.

<sup>b</sup>Reference 25.

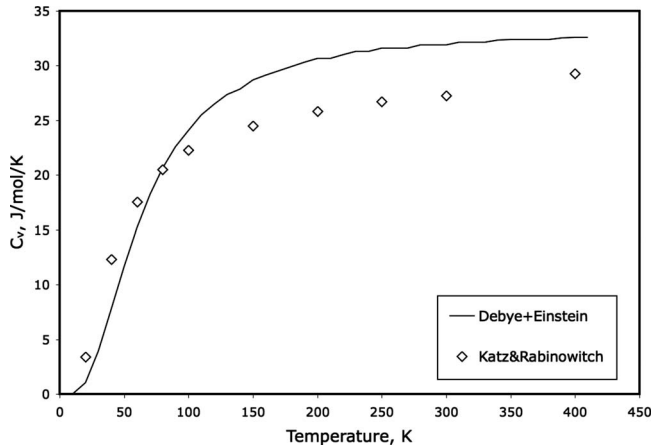


FIG. 3. Specific heat  $C_v$  (J/mol K) calculated using the Einstein and/or Debye models for  $\alpha$ -uranium and the data given in Table III (solid line), compared to the data compiled in Ref. 13 (open diamonds).

currently outside the reach of modern electronic structure theory.

In order to consider the Einstein contribution to the thermodynamic properties of solid  $\alpha$ -uranium, the local vibrational properties of the uranium atoms must be considered. The local vibrational modes obtained for  $\alpha$ -uranium under the constraint that only one uranium atom in the 96 atom supercell is allowed to vibrate (coupled atomic vibrations are not considered) have frequencies of 79, 104, and 106  $\text{cm}^{-1}$  (Table III). In terms of vibrational energy, the modes are found at 9, 12.5, and 12.7 meV. Inspection of the phonon DOS presented in Ref. 27 shows peaks at these values for the spectra obtained at 433 and 655 K, with a stronger contribution near 12.5 eV occurring due to overlap between the two latter modes. At lower temperatures, these modes are not as noticeable, and this may be a result of the phonon softening and influence of the charge-density wave transitions occurring in  $\alpha$ -uranium (this transition leads to a modification of the lattice positions, and therefore, a somewhat different unit cell). As noted in Ref. 27 significant progress is still required in first-principles techniques to understand the electronic contribution to the variation in atomic force constants with temperature, and the resulting impact upon phase entropies and phase transitions. This is reflected by the discrepancy between the specific heat curves calculated based on compiled experimental data,<sup>13</sup> and those determined using the current model, as displayed in Fig. 3. It can be seen that the density functional model presented here leads to underestimated specific heats at low temperature and overestimated specific heats at higher temperatures with the crossover point occurring at about 80 K.

#### Energies of vacancy formation and phase transformations

Next, I consider the calculation of some materials defect properties and phase change energies. In Table IV, I presented the vacancy formation energy and fcc and/or bcc energies relative to the  $\alpha$ -uranium phase. The vacancy forma-

TABLE IV. Theoretically calculated values for the vacancy formation energy in  $\alpha$ -uranium (unrelaxed in parentheses)  $E_v^f$  and the fcc/bcc/ $\alpha$ -uranium energy differences,  $E_{\text{fcc}} - E_\alpha$  and  $E_{\text{bcc}} - E_\alpha$ , respectively, given in eV, calculated using the scalar-relativistic and spin-orbit PAW methods, the full-potential (all-electron) technique of Söderlind (Ref. 3), and the pseudopotential method of Crocombette *et al.* (Ref. 6).

	$E_v^f$	$E_{\text{fcc}} - E_\alpha$	$E_{\text{bcc}} - E_\alpha$
SR	1.95 (2.20)	0.39	0.27
SOC		0.35	0.24
FP		0.26	0.22
PP		0.22	0.16

tion energy as calculated in the scalar-relativistic approximation using the gamma point only calculation and a 96-atom unit cell is 2.20 eV without atomic relaxation and 1.95 eV with atomic relaxation. This value is significantly higher than the vacancy formation energies reported for other metals and higher than literature estimates for this parameter. The positron annihilation experiments described in Ref. 28, for example, yield a minimum for the vacancy formation energy of 1 eV and estimate the energy to be  $1.20 \pm 0.25$  eV. The authors furthermore state that a value larger than 1.3 eV is unlikely. The energy obtained from the PAW calculations is therefore significantly higher than the estimates obtained from the positron-annihilation experiments. In general, however, the literature for vacancy energies in uranium is scarce.

Comparison to the calculated value for a neighboring element, plutonium in the  $\delta$  phase, also indicates that the calculated vacancy energy for uranium is particularly high:  $E_f^v$  for  $\delta$ -plutonium ranges between 1.4 and 1.6 eV.<sup>29</sup> Calculations using larger supercells, a more refined  $k$ -point mesh or spin-orbit coupling may lead to refinements of this energy; however, they are unlikely to be on the order of several tenths of an eV. Due to the apparent ambiguities of the interpretation of the positron annihilation experiment,<sup>28</sup> it is suggested that more experimental work is required to complement further efforts to refine this value using theoretical means.

The phase transition energies are overestimated in the scalar-relativistic approximation by 0.04 and 0.03 eV for fcc and bcc, respectively. Both sets of values are larger than those obtained in previous calculations (full potential and hard pseudopotential) and more particularly so for the fcc energy. It is not immediately clear which set of energy differences is more accurate, as there are no experimental numbers to compare to for this (unphysical) transformation (although it will be important for multiscale method development). From a theoretical viewpoint, the full-potential results should be considered to provide the most accurate energy differences currently available, and hence, the PAW method appears to be overestimating the energy of the bcc and fcc phases, relative to the orthorhombic alpha phase (calculations made at higher  $k$ -point meshes and energy cutoffs did not change the results).

TABLE V. Surface energy  $\gamma$  (J/m<sup>2</sup>) and surface relaxation given in absolute interlayer distances (Å) as well as percent expansion for model  $N$ -layer  $\alpha$ -uranium (001) oriented slabs.  $d_{12}$  is the outermost interlayer distance and  $d_{23}$  the second-outermost interlayer distance in the (001) direction. The distances given in parentheses were fixed at the bulk constants for  $N=3-5$ . The difference in energy  $-\Delta E_{\text{mag}}$  between magnetic and nonmagnetic calculations is also given per surface atom (meV), as well as the magnetization per surface atom ( $\mu/\mu_B$ ), for this work and Ref. 33. The work function  $\Phi$  is also given in eV.

$N$	$d_{12}$	$d_{12}\%$	$d_{23}$	$d_{23}\%$	$\gamma$	$-\Delta E_{\text{mag}}$ ( $\mu/\mu_B$ )				$\Phi$
						This work	Ref. 33	This work	Ref. 33	
3	2.337	-4.5	(2.447)	0.0	1.427	3	11	0.88	0.66	3.58
4	2.360	-3.5	(2.447)	0.0	1.408	2		0.67		3.59
5	2.361	-3.5	(2.447)	0.0	1.396	5	16	0.63	0.65	3.64
6	2.364	-3.4	2.480	1.4	1.388	4		0.48		3.82
7	2.358	-3.6	2.472	1.0	1.383	2	20	0.55	0.65	3.63

### Properties of the (001)-oriented $\alpha$ -uranium single-crystal surface

Very often, material transformations begin with the alteration of the material at its interface with some environment. As a precursor to studying surface phenomena on uranium surfaces and specifically single-crystal surfaces, the properties of the (001) surface have been calculated in the scalar relativistic approximation using the projector-augmented wave treatment. To the best of the author's knowledge, there are no estimates of the structural and thermodynamic properties of the (001) surface of  $\alpha$ -uranium available in the literature. Hence, much of the data presented in Table V is currently without validation, with the exception of some estimates available based on the properties of polycrystalline  $\alpha$ -uranium surfaces, and the validation provided already in the form of successful modeling of the properties of the bulk crystalline material.

Estimates of the surface energy of polycrystalline uranium range between 1.000 and 1.490 J/m based on theoretical correlations between physical parameters such as the heat of sublimation and atomic volume.<sup>3,30</sup> An investigation of fission bubbles in  $\alpha$ -uranium yielded an approximate surface energy of  $1.0 \pm 0.5$  J/m.<sup>2,31</sup> The surface energy arising from the present PAW calculations of 1.4 J/m<sup>2</sup> clearly falls within this range.

Thermionic experiments described in Ref. 32 report a work function for polycrystalline uranium of  $3.47 \pm 0.03$  eV, which is close to the 3.6 eV obtained for the (001) single-crystal surface examined in this work. The higher value of 3.8 eV obtained for the six-layer slab is likely an anomaly arising from the fact that the six-layer simulation contained only 2.5 equivalent layers of vacuum, compared to the approximately five equivalent layers used in the other simulations.

The energy difference between the ferromagnetic and nonferromagnetic surfaces ( $\Delta E_{\text{mag}}$ ) obtained in the scalar relativistic calculations reported in Table V are significantly smaller (by an order of magnitude) than the energy differences calculated using the spin-orbit, full-potential calculations obtained by Stojić *et al.*<sup>33</sup> While this may arise from the difference in computational method applied [spin-orbit coupling and all-electron (full-potential) treatment versus scalar

relativistic and/or projector-augmented wave], there is no experimental evidence for strongly magnetic properties of the  $\alpha$ -uranium surface. Furthermore, the results reported in Ref. 33 were obtained by calculations performed on the *unrelaxed* (100) surfaces. Surface relaxation is likely to reduce the magnetic moment as bonding between the outermost uranium atoms is enhanced via the contraction (see next paragraph). The calculated spin moments on the surface atoms are qualitatively similar, but again, not in quantitative agreement. Further theoretical and experimental investigations of the magnetic surface properties of uranium are required to elucidate this issue, which includes fully relaxed, spin-orbit, and full-potential calculations. Either way, the energy differences are small, and hence, any magnetic properties would exist only at temperatures below  $\sim 250$  K (calculated using the larger energy difference reported for the seven-layer slab in Ref. 33). For the purposes of engineering systems and materials, design effects at temperatures significantly below room temperature are typically not of great concern.

The surface relaxations obtained by PAW density functional theory are consistent with the typical behaviors of metals. In general, the outermost layer of a metallic surface contracts by an amount  $<10\%$  and the subsurface (second outermost) layer will expand according to bond-order conservation ideas<sup>34</sup> (stronger bonding to the outer layer will lead to weakened bonding with the third outermost layer). The PAW calculations determine an external relaxation for the (001) surface of  $\alpha$ -uranium of  $\sim -3.5\%$  and a subsurface relaxation of  $\sim +1\%$ . Experiments such as low-energy electron diffraction performed on the (001) single-crystal uranium surface would be useful for validating the use of the scalar-relativistic PAW calculations for determining these relaxation parameters. However, to our knowledge, no such experiments have been reported in the literature.

By utilizing the model of Hayes *et al.*,<sup>14</sup> it is possible to relate the (001) surface energy ( $\gamma=1.4$  J/m<sup>2</sup>), the bulk-interlayer distance ( $d=2.447$  Å), and the  $c_{33}$  elastic constant ( $c_{33}=331$  GPa, this work) to the cohesive properties of the (001) planes. Succinctly, this model imposes the crack formation criterion that the elastic strain energy imposed upon an elongated crystal must exceed the surface energy of the crystal. Thus, at some elongation, surface formation via crack development must become more favorable than con-

tinuously straining the crystal. Two parameters arise from this model: the critical elongation and the stress required to achieve that elongation (critical peak traction). Although  $\alpha$ -uranium is a metal and will fail via plastic deformation (movement of dislocations) the brittle fracture value provides a guide to the “yield stress” of the material, at which point the elastic limit is reached and plastic modes will take over. The important modes of failure via plastic deformation modes and/or intergranular cracking could be modeled at a later stage using interatomic pair-potential techniques. The simple elastic model presented by Hayes *et al.*<sup>14</sup> determines the critical crack opening displacement by equalizing the elastic energy density imposed by a critical strain value to the surface energy yielded upon complete fracture. The procedure is analogous to the Griffith equation for crack propagation.<sup>35</sup> The resulting critical opening displacement is  $\bar{\delta}_r = 2\sqrt{\gamma w/c_{33}}$ , where  $w$  is the sample width. As such, the critical crack opening is dependent on the sample width, as the elastic strain energy is a volume property, compared to the surface energy, which is a two-dimensional surface quantity. For a 10  $\mu\text{m}$  single crystal, therefore, in the absence of dislocations, brittle failure would occur at a critical displacement of 130  $\text{\AA}$ . The related critical peak traction is  $\bar{\sigma}_r = c_{33}\bar{\delta}_r/w$  or 431 MPa for a 10  $\mu\text{m}$  single-crystal. The computed value is closer to the value determined by Hayes *et al.* for the  $\alpha$ - $\text{Al}_2\text{O}_3$  single crystal than that for Al(111), consistent with the semiplasticity (rather than total plasticity) of  $\alpha$ -uranium as it indicates that the metal is more similar to the aluminum oxide than the aluminum metal.<sup>13,14</sup> Reference 13 cites a reported yield stress of 345 MPa for polycrystalline  $\alpha$ -uranium, comparable with the 387 MPa obtained using the measured room temperature  $c_{33}$  and the above equation.

### CONCLUSIONS

After considering a number of materials and surface properties for  $\alpha$ -uranium, it can be seen that the projector-augmented wave formalism is able to predict properties that are in reasonable agreement with experiment, comparable to the results from full-potential calculations. The calculated vacancy formation energy is higher than expected, and this points to a need for further theoretical and experimental scrutiny. The PAW methodology allows calculation simulation cells consisting of at least 100 atoms, and therefore, allows investigation of phenomena such as impurities and vacancies, with an accuracy that has been demonstrated to be comparable to that obtained by all-electron, full-potential methods. Furthermore, the PAWs used in this work have been demonstrated to have greater accuracy and a lower required energy cutoff than pseudopotentials used in previous work,

providing both accuracy and computational gains.

The temperature dependence of the force constants, and hence the moduli and Debye temperature, remains a case for further theoretical investigation. These problems are not unique to the PAW method employed in this work. The results of the PAW calculations are indeed very close to those obtained by full-potential methods; however, both approaches are limited to 0 K predictions and do not capture the electronic thermal-excitation contributions to the force constants. Hence, a major advancement in the application of basic electronic structure theory is still required to investigate this problem, and the related problems of phase diagrams and equations of state.

The surface energies and work functions calculated using this approach are in good agreement with estimates from the literature. Furthermore, a slight preference for surface magnetization is observed, consistent with the results of unrelaxed full-potential calculations, although this is at the limits of the calculation’s self-consistency. Experimental validation of the predicted surface-relaxation constants obtained in this work would be useful.

The choice of spin-orbit versus scalar-relativistic modeling of the relativistic effects in  $\alpha$ -uranium is seen to cause only slight differences in the quantitative results obtained using the PAW formalism. However, as it is not known in which cases the spin-orbit coupling component will be most important, theoretical investigations should still be performed using both techniques, where possible, until a consensus is reached.

Finally, it should be emphasized that the evaluation of uranium materials properties using density functional theory is of sufficient accuracy to begin to probe many materials and chemical interactions for the purpose of understanding the fundamental atomic contribution to transitions occurring under service conditions of this material and to be used as a basis for the construction of multiscale models capable of modeling transformations involving lower symmetry materials features such as grain boundaries, dislocations, and surfaces.

### ACKNOWLEDGMENTS

The Los Alamos National Laboratory is operated by Los Alamos National Security LLC for the National Nuclear Security Administration of the U.S. Department of Energy under Contract No. DE-AC52-06NA25396. The author thanks Scott Lillard, Srinivasa Srivilliputhur, and Bogdan Mihaila for their technical expertise and assistance. The support of Roland Schulze, David Teter, and Thomas Zocco of the Enhanced Surveillance Project is also acknowledged.

<sup>1</sup>M. E. Eberhart and D. P. Clougherty, *Nat. Mater.* **3**, 659 (2004).

<sup>2</sup>W. A. Curtin and R. E. Miller, *Modell. Simul. Mater. Sci. Eng.* **11**, R33 (2003).

<sup>3</sup>P. Söderlind, *Phys. Rev. B* **66**, 085113 (2002).

<sup>4</sup>C. S. Barrett, M. H. Mueller, and R. L. Hitterman, *Phys. Rev.* **129**, 625 (1963).

<sup>5</sup>A. C. Lawson, B. Martinez, J. A. Roberts, B. I. Bennett, and J. W. Richardson, Jr., *Philos. Mag. B* **80**, 53 (2000).

- <sup>6</sup>J. P. Crocombette, F. Jollet, L. T. Nga, and T. Petit, *Phys. Rev. B* **64**, 104107 (2001).
- <sup>7</sup>K. Balasubramanian, W. J. Siekhaus, and W. McLean II, *J. Chem. Phys.* **119**, 5889 (2003).
- <sup>8</sup>L. Fast, O. Eriksson, B. Johansson, J. M. Wills, G. Straub, H. Roeder, and L. Nordström, *Phys. Rev. Lett.* **81**, 2978 (1998).
- <sup>9</sup>P. E. Blöchl, O. Jepsen, and O. K. Andersen, *Phys. Rev. B* **49**, 16223 (1994).
- <sup>10</sup>D. Vanderbilt, *Phys. Rev. B* **41**, 7892 (1990).
- <sup>11</sup>G. Kresse and D. Joubert, *Phys. Rev. B* **59**, 1758 (1999).
- <sup>12</sup>G. Kresse and J. Furthmüller, *Phys. Rev. B* **54**, 11169 (1996).
- <sup>13</sup>J. J. Katz and E. Rabinowitch, *The Chemistry of Uranium: The elements, Its binary and Related Compounds* (Dover, New York, 1961).
- <sup>14</sup>R. L. Hayes, M. Ortiz, and E. A. Carter, *Phys. Rev. B* **69**, 172104 (2004).
- <sup>15</sup>J. P. Perdew, J. A. Chevary, S. H. Vosko, K. A. Jackson, M. R. Pederson, D. J. Singh, and C. Fiolhais, *Phys. Rev. B* **46**, 6671 (1992).
- <sup>16</sup>H. J. Monkhorst and J. D. Pack, *Phys. Rev. B* **13**, 5188 (1976).
- <sup>17</sup>M. Methfessel and A. T. Paxton, *Phys. Rev. B* **40**, 3616 (1989).
- <sup>18</sup>S. K. Joshi, *Phys. Rev.* **121**, 40 (1961).
- <sup>19</sup>Probably a higher  $k$ -point mesh should be used to achieve convergence with respect to  $k$  points; however, the present computational resources do not allow it.
- <sup>20</sup>E. Jahnke and F. Lösch, *Tables of Higher Functions* (McGraw-Hill, New York, 1960).
- <sup>21</sup>B. Blumenthal and J. E. Sanecki, *J. Nucl. Mater.* **22**, 100 (1967).
- <sup>22</sup>F. H. Spedding and B. J. Beaudry, *J. Less-Common Met.* **25**, 61 (1971).
- <sup>23</sup>G. H. Lander, E. S. Fisher, and S. D. Bader, *Adv. Phys.* **43**, 1 (1994).
- <sup>24</sup>A. S. Wilson and R. E. Rundle, *Acta Crystallogr.* **2**, 126 (1949).
- <sup>25</sup>E. S. Fisher and H. J. McSkimin, *J. Appl. Phys.* **29**, 1473 (1958).
- <sup>26</sup>P. Söderlind, *Adv. Phys.* **47**, 959 (1998).
- <sup>27</sup>M. E. Manley, B. Fultz, R. J. McQueeney, C. M. Brown, W. L. Hults, J. L. Smith, D. J. Thoma, R. Osborn, and J. L. Robertson, *Phys. Rev. Lett.* **86**, 3076 (2001).
- <sup>28</sup>H. Matter, J. Winter, and W. Triftshäuser, *J. Nucl. Mater.* **88**, 273 (1980).
- <sup>29</sup>G. Robert, A. Pasturel, and B. Siberchicot, *Europhys. Lett.* **71**, 412 (2005).
- <sup>30</sup>J. W. Taylor, *Metallurgica* **50**, 161 (1954).
- <sup>31</sup>J. E. Bainbridge and B. Hudson, *J. Nucl. Mater.* **17**, 237 (1965).
- <sup>32</sup>E. G. Rauh and R. J. Thorn, *J. Chem. Phys.* **31**, 1481 (1959).
- <sup>33</sup>N. Stojić, J. W. Davenport, M. Komelj, and J. Glimm, *Phys. Rev. B* **68**, 094407 (2003).
- <sup>34</sup>E. Shustorovich, *Surf. Sci. Rep.* **6**, 1 (1986).
- <sup>35</sup>A. A. Griffith, *Philos. Trans. R. Soc. London, Ser. A* **221**, 163 (1920).